IEEE Access
Multidisciplinary | Rapid Review | Open Access Journal

Received November 1, 2016, accepted November 23, 2016, date of publication December 2, 2016,
date of current version February 25, 2017.

Digital Object Identifier 10.1109/ACCESS.2016.2634096

Resource Allocation for Transmit Hybrid Beamforming in Decoupled Millimeter Wave Multiuser-MIMO Downlink

IRFAN AHMED[1], (Senior Member, IEEE), HEDI KHAMMARI[1], AND ADNAN SHAHID[2], (Member, IEEE)
[1]Computer Engineering Department, Taif University, Ta'if 21974, Saudi Arabia
[2]Department of Information Technology, Ghent University, 9000 Ghent, Belgium

Corresponding author: I. Ahmed (irfan.ahmed@ieee.org)

This work was supported by the King Abdulaziz City for Science and Technology under Grant PC-35-144.

ABSTRACT This paper presents a study on joint radio resource allocation and hybrid precoding in multi-carrier massive multiple-input multiple-output communications for 5G cellular networks. In this paper, we present the resource allocation algorithm to maximize the proportional fairness (PF) spectral efficiency under the per subchannel power and the beamforming rank constraints. Two heuristic algorithms are designed. The proportional fairness hybrid beamforming algorithm provides the transmit precoder with a proportional fair spectral efficiency among users for the desired number of radio-frequency (RF) chains. Then, we transform the number of RF chains or rank constrained optimization problem into convex semidefinite programming (SDP) problem, which can be solved by standard techniques. Inspired by the formulated convex SDP problem, a low-complexity, two-step, PF-relaxed optimization algorithm has been provided for the formulated convex optimization problem. Simulation results show that the proposed suboptimal solution to the relaxed optimization problem is near-optimal for the signal-to-noise ratio $SNR \leq 10$ dB and has a performance gap not greater than 2.33 b/s/Hz within the SNR range 0–25 dB. It also outperforms the maximum throughput and PF-based hybrid beamforming schemes for sum spectral efficiency, individual spectral efficiency, and fairness index.

INDEX TERMS Millimeter-wave, beamforming, 5G, resource allocation.

I. INTRODUCTION

Recently, the need for high data rates has dramatically increased. The 4G or Long Term Evolution-Advanced (LTE-A) technology can handle applications with data rates up to several Mbps. Therefore, new mobile applications that mandate data rates in the range of several Gigabits per second (Gbps) cannot be handled with such technology. To handle such large data volumes, higher frequency bands spans from 6 to 95 GHz must be employed [1], [2]. 5G wireless technology will use these frequency bands which leads to the emergence of prominent technology by 2020 [3]. Moreover, 5G mobile technology shall comply with predecessor technologies, similar to LTE-A technology, which is backward compatible with previous generations [4].

The massive multiple-input multiple-output (MIMO) systems permit high spectral efficiency by using large antenna arrays at both the transmitter and the receiver of a wireless communication link. The large spectrum available in the millimeter-wave bands presents an emerging alternative to the traditional wireless systems to achieve several fold mobile data traffic increase. The millimeter wave (mmWave) systems are designed to overcome signal attenuation and to provide high throughput wireless communication links. In mmWave systems, the beamforming uses a large antenna arrays to overwhelm path loss with directional transmission. In Massive MIMO systems, the traditional baseband digital beamforming (DB) requires one distinct radio-frequency (RF) chain per antenna. Both beamforming and precoding are done at baseband, however in mmWave systems, the high power consumption and the high cost of mixed-signal and RF chains led to opt to hybrid beamforming (HB) operating in the baseband and analog domains. Thus several studies proposed different architectures aiming to reduce the number of RF chains by combining an analog RF beamformer and a baseband digital beamformer. Such techniques are known as hybrid beamforming methods.

Hybrid beamforming methods are devoted to jointly optimize the analog and digital beamformers to maximize the achievable rate. The performances of the different hybrid beamforming algorithms can be compared in light of power consumption calculations and achievable rates. A user scheduling and sub-carrier allocation algorithm for multiuser downlink MIMO orthogonal frequency division multiple access (OFDMA) systems with hybrid analog-digital beamforming was proposed in [5]. Such a design with hybrid analog-digital beamforming algorithm was designed to reduce the number of RF chains and Phase Shifters (PS). The subsequent beamforming system should achieve the same performance of a digital beamforming that uses the same number of RF chains as the number of antennas of the transmitter. A transceiver design for maximizing the spectral efficiency of a large-scale MIMO system with hybrid beamforming architecture using a limited number of RF chains and finite-resolution PSs was proposed in [6]. It was shown that for the critical case where the number of RF chains is equal to the number of data streams, the performance is close to that of the exhaustive search method. The achievable rate can be improved significantly by adding extra RF chains in low-resolution PS case. A hybrid beamforming structure reported in [7], led to obtain the same performance as the fully-digital beamforming scheme if the number of RF chains at each end is greater than or equal to twice the number of data streams. In [8], a different hybrid architecture replaced the PSs with switches at the receiver and showed that antenna selection is preferred in a range of operating conditions. This architecture of hybrid beamforming was presented for compressed sensing based channel estimation. An iterative hybrid transceiver design algorithm based on the nonlinear least-squares formulation for mmWave MIMO systems was presented in order to reduce the performance gap between the optimal full-baseband and the existing Orthogonal Matching Pursuit (OMP)-based hybrid transceiver designs in spite of using a much smaller number of RF chains [9]. A practical transmitter structure in which each antenna is only connected to a unique RF chain, was designed to optimize the analog and digital beamforming matrices for a maximum achievable rate with transmit power constraint. For a small antenna array or for a great number of propagation paths, the performance of such method can be improved by adjusting analog amplitude to reduce the complexity [10]. A hybrid beamforming based multi-beam transmission diversity scheme was proposed for a single stream transmission for single user MIMO operation. The proposed structure flexibility permitted to adaptively adjust the transmission signal according to the unfavorable channel characteristics at high frequency bands including mmWave [11].

Compress sensing and matching pursuit are popular approaches to find the near optimal precoders and combiners. A precoding strategy using a variant of matching pursuit was considered to develop an iterative hybrid beamforming algorithm for the single user mmWave channel. The proposed solution assumes only partial channel knowledge at both the base and mobile stations in the form of angle of arrival (AoA) knowledge. The presented precoding method utilizes the channel sparsity, reciprocity, and the algorithmic concept of basis pursuit [12]. For a single user beamforming and precoding in mmWave systems with large arrays, a low hardware complexity precoding solution considered the precoder design problem as a sparsity constrained least squares problem. The proposed algorithm allows mmWave systems to approach waterfilling capacity [13]. An inclusive survey on the beamforming in millimeter wave communications is presented in [14].

Motivation: The DB is an optimal precoder for any design criterion and channel model [7], [15]. Using maximum throughput or proportional fairness (PF) criteria, one can design an optimal maximum throughput digital beamformer (MTDB) or PF digital beamformer (PFDB). DB based designs need one RF chain per antenna. Due to the higher cost and the power consumption in massive MIMO mmWave communication systems (because of large number of RF chains, containing digital to analog converter (DAC), data converter, mixer etc [16]), DB is not feasible for practical implementations. HB is the feasible choice to achieve the acceptable performance. A general approach for hybrid precoders design is to maximize the spectral efficiency by minimizing the Frobenius norm of the difference between the digital precoder and the proposed hybrid precoder using basis pursuit [15], [16]. In most of the aforementioned HB designs either the objective is to minimize the number of RF chains [5], [8], [9], or to maximize the throughput for limited number of RF chains [6], [7], [10], [13], [15]. In a practical cellular networks, fairness among the equally paying users is an utmost important deployment and optimization criterion. PF is a widely adopted radio resource allocation scheme in access networks [17]. There is no such literature that provides PF-based hybrid precoder for a desired number of RF chains. PF-based systems with the choice of number of RF chains give upper bound on the achievable system PF throughput tradeoff with capital and running costs. To date, the optimal solution for a given number of RF chains in HB design is still an open research topic [14], [18].

Objectives: To develop a transmit precoder that maximizes the PF spectral efficiency for a given number of RF chains and per subchannel power constraint in multiuser multicarrier massive MIMO system.

Contributions: The contribution of this paper is threefold:

1) HB precoder design for PF-based resource allocation for multiuser and multicarrier massive MIMO systems. It has been shown that for low signal-to-noise ratio (SNR) values with 64 transmit antennas, 8 users with single antenna, and 16 RF chains, the PF hybrid beamforming (PFHB) provides a comparative average sum spectral efficiency with respect to maximum throughput hybrid beamforming (MTHB) with upto 50% increase in fairness when the users are 50m apart.
2) We have transformed the non-convex rank-constraint resource allocation problem to the form of convex

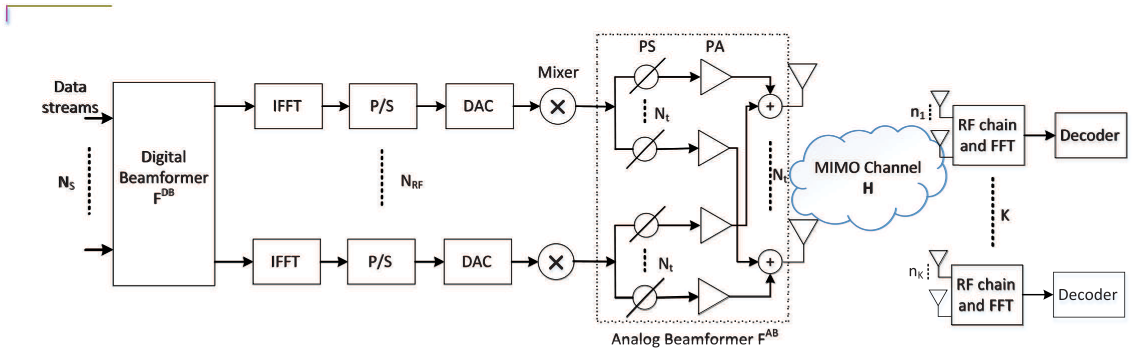

FIGURE 1. A transmit and receive structure of hybrid beamforming in multicarrier multiuser systems.

optimization problem which can be solved by standard semidefinite programming (SDP) techniques. In particular, the non-convex rank constraint has been replaced by 2-norm and trace constraint. The nuclear norm is used as a convex substitute in the objective function because it is the convex envelope of the rank.

3) A low complexity, subchannel level PF relaxed optimization (PFRO) solution is presented for feasible implementations. It solves the convex optimization problem in two steps. The first step provides the optimal users' combinations and power allocations, whereas, the second step extracts the precoder with the desired number of RF chains. Simulation results show that PFRO outperforms the MTHB and PFHB in average sum spectral efficiency, individual user spectral efficiency, and the fairness index.

This paper is organized as follows: In section II we present the system model. Section III is about the problem formulation and performance analysis of hybrid beamforming based on proportional-fair spectral efficiency in mmWave MU-MIMO downlink. Performance evaluation and comparisons of proposed scheme are provided in section IV, followed by conclusions in section V.

Notations: Vectors and matrices are represented by boldface lower-case and upper-case letters, respectively, other notations are explained below:

$\mathbb{C}^{m\times n}$	$m \times n$ dimensional complex space
$\mathcal{K}$	Caligraphic letters denote sets
$tr(\mathbf{A})$	Trace of matrix $\mathbf{A}$
$blkd(\cdot)$	Block diagonal
$\mathbf{A}^T$	$\mathbf{A}$ transpose
$\mathbf{A}^H$	$\mathbf{A}$ conjugate transpose
$\mathbb{E}(\mathbf{A})$	Expected value of $\mathbf{A}$
$\mathbf{I}_n$	Identity matrix of size $n \times n$
$\|\mathbf{A}\|_*$	Nuclear norm of matrix $\mathbf{A}$
$\|\mathbf{A}\|_2$	2-norm of matrix $\mathbf{A}$
$\|\mathbf{A}\|_F$	Frobenius norm of matrix $\mathbf{A}$

II. SYSTEM MODEL

We consider a multiuser MIMO cellular system in which the eNB with N_t antennas sends N_s data streams to K number of UEs each equipped with n_k antennas as shown in Fig. 1. We denote N_r as the sum of the antennas on all UEs such that $N_r = \sum_{k=1}^{K} n_k$. Perfect channel state information (CSI) is assumed at eNB and each UE. We use orthogonal frequency division multiple access (OFDMA) block-based transmission because this is the modulation of choice of modern cellular and wireless local area networks [19]. We assume narrowband block fading such that each OFDM block contains N_s symbols and N_f subchannels. Then, the OFDM block becomes

$$\mathbf{S} = \begin{bmatrix} s_{1,1} & s_{1,2} & \cdots & s_{1,N_f} \\ s_{2,1} & s_{2,2} & \ddots & \vdots \\ \vdots & \ddots & \ddots & s_{N_s-1,N_f} \\ s_{N_s,1} & \cdots & s_{N_s,N_f-1} & s_{N_s,N_f} \end{bmatrix} \tag{1}$$

We make $N_s = K$, i.e., the number of symbols is equal to the number of UEs. The transmitter uses an $N_{RF} \times N_s$ digital beamformer $\mathbf{F}_i^{DB}$ for each subchannel i, followed by an $N_t \times N_{RF}$ analog beamformer $\mathbf{F}_i^{AB}$ for each subchannel i. The sampled transmitted block on subchannel i is given by

$$\mathbf{x}_i = \mathbf{F}_i^{AB}\mathbf{F}_i^{DB}\mathbf{s}_i \tag{2}$$

where $\mathbf{x}_i$ is an $N_t \times 1$ column vector and $\mathbf{s}_i = [s_{1,i}, \ldots, s_{K,i}]^T$. The transmitted symbol for UE k on subchannel i, $x_{k,i}$ is a linear function of symbols, i.e., $x_{k,i} = \mathbf{F}_i^{AB}\mathbf{f}_{k,i}^{DB}s_{k,i}$, where $\mathbf{f}_{k,i}^{DB}$ is the k^{th} column of $\mathbf{F}_i^{DB}$. The transmitted OFDM block is $\mathbf{x} = [\mathbf{x}_1, \ldots, \mathbf{x}_{N_f}]$.

In general, MIMO channel models fall into two categories: (i) analytical models, and (ii) geometrical models. Analytical models describe the channel transfer function matrix, whereas, geometrical channel models describe the physical propagation between transmit array and receive array [19].

A. ANALYTICAL CHANNEL MODEL

The input-output relationship of the system model is given by

$$\mathbf{y} = \mathbf{H}\mathbf{x} + \mathbf{w} \tag{3}$$

where $\mathbf{x} = [\mathbf{x}_1, \ldots, \mathbf{x}_{N_f}]^T$ is the transmit signal vector, $\mathbf{H} = blkd(\mathbf{H}_1, \ldots \mathbf{H}_{N_f})$ is the system channel matrix, $\mathbf{w} \in \mathbb{C}^{N_f N_r \times 1}$ is the noise vector, and $\mathbf{y} = [\mathbf{y}_1, \ldots, \mathbf{y}_{N_f}]^T$ is the receive signal vector. The received signal $\mathbf{y}_i$ on the i^{th} subchannel can be obtained from (3) as

$$\mathbf{y}_i = \mathbf{H}_i \mathbf{x}_i + \mathbf{w}_i \tag{4}$$

where $\mathbf{H}_i = [\mathbf{H}_{1,i}, \ldots, \mathbf{H}_{K,i}]^T \in \mathbb{C}^{N_r \times N_t}$ is the channel matrix with $\mathbf{H}_{k,i} = [\mathbf{h}_{1,k}, \ldots, \mathbf{h}_{n_k,k}]^T$, $\mathbf{x}_i$ is given in (2), and $\mathbf{y}_i = [\mathbf{y}_{1,i}, \ldots, \mathbf{y}_{K,i}]^T$. On the i^{th} subchannel, the j^{th} UE receives the sum of all transmitted signals for K UEs over its MIMO channel $\mathbf{H}_{j,i}$ as

$$\mathbf{y}_{j,i} = \sum_{k=1}^{K} \mathbf{H}_{j,i} \mathbf{x}_{k,i} + \mathbf{w}_{j,i} \tag{5}$$

where $\mathbf{y}_{j,i}$ is an $n_j \times 1$ vector, $\mathbf{H}_{j,i} \in \mathbb{C}^{n_j \times N_t}$ is the MIMO channel matrix which is defined in the next subsection. We denote the rank of the channel matrix $\mathbf{H}_{j,i}$ by $r_{j,i}$, where $0 \leq r_{j,i} \leq \min(n_j, N_t)$, $\forall i$. In matrix form, the above equation is given as

$$\mathbf{y}_{j,i} = \mathbf{H}_{j,i} \mathbf{x}_i + \mathbf{w}_{j,i} \tag{6}$$

The $n_k \times N_f$ received signal at the k^{th} UE is given by

$$y_k = [\mathbf{H}_{k,1} \mathbf{F}_1^{AB} \mathbf{F}_1^{DB} \mathbf{s}_1, \ldots, \mathbf{H}_{k,N_f} \mathbf{F}_{N_f}^{AB} \mathbf{F}_{N_f}^{DB} \mathbf{s}_{N_f}] \mathbb{F}^{-1} + \mathbf{w}_k, \tag{7}$$

where $\mathbf{H}_{k,i} \in \mathbb{C}^{n_k \times N_t}$ is the random MIMO channel between eNB and UE k for the i^{th} subchannel, $\mathbf{x}_i = \mathbf{F}_i^{AB} \mathbf{F}_i^{DB} \mathbf{s}_i$ is $N_t \times 1$ transmit signal vector, $\mathbb{F}^{-1}$ is the inverse fast fourier transform (IFFT) matrix of size N_f, and $\mathbf{w}_k \sim \mathcal{CN}(0, \boldsymbol{\sigma}^2)$ is the $N_f \times 1$ vector of additive white Gaussian noise (AWGN) of which each element follows complex normal distribution with zero mean and variance σ^2.

Combining the signals for all UEs in a K dimensional received signal vector $\mathbf{y} = [\mathbf{y}_1, \ldots, \mathbf{y}_K]$, we get the system equation as

$$\mathbf{y} = \mathbf{H} \mathbf{F}^{AB} \mathbf{F}^{DB} \mathbf{S} \mathbb{F}^{-1} + \mathbf{w}, \tag{8}$$

The FFT operation at the UE k transforms the received signal into frequency domain as

$$\acute{\mathbf{y}}_k = [\mathbf{H}_{k,1} \mathbf{F}_1^{AB} \mathbf{F}_1^{DB} \mathbf{s}_1, \ldots, \mathbf{H}_{k,N_f} \mathbf{F}_{N_f}^{AB} \mathbf{F}_{N_f}^{DB} \mathbf{s}_{N_f}] + \mathbf{w}_k \mathbb{F}. \tag{9}$$

B. GEOMETRICAL CHANNEL MODEL

Due to the high free-space pathloss characteristic at mmWave frequencies, mmWave propagation leads to limited spatial scattering. In addition, the large tightly-packed antenna arrays that are characteristic of mmWave transceivers lead to high levels of antenna correlation. This combination of sparse scattering and tightly packed antenna arrays makes many of the statistical fading distributions (e.g., iid Rayleigh fading model) used in traditional MIMO analysis inaccurate for mmWave channel modeling. Therefore, we adopt a narrowband channel representation, based on the extended Saleh-Valenzuela model, which accurately captures the mathematical structure present in mmWave channels [7], [20]. For simplicity, we assume that each scattering cluster around the transmitter and receiver contributes a single propagation path [13]. Geometrical channel model describes the physical propagation between transmit array and receive array. Due to near optical line-of-sight (LOS) wave propagation at mmWave frequencies, the mmWave channels are expected to have limited scattering, say, L. The mmWave MIMO channel matrix with N_t transmit and N_r receive antennas, can be modeled as

$$\mathbf{H} = \sqrt{\frac{N_t N_r}{\rho L}} \sum_{l=1}^{L} \alpha_l \mathbf{a}_t(\phi_{t,l}) \mathbf{a}_r^H(\phi_{r,l}), \tag{10}$$

where α_l represents the complex gain of the l^{th} path with i.i.d. $\mathcal{CN}(0, 1)$ and ρ is the distance dependent pathloss between transmitter and receiver is taken from [21]. Moreover, $\mathbf{a}_t$ and $\mathbf{a}_r$ are the transmit and receive steering vectors, respectively. The variables $\phi_{t,l} \in [0, 2\pi)$ and $\phi_{r,l} \in [0, 2\pi)$ are the l^{th} path's azimuth angles (boresight angles in the transmit array and receive array) of departure and arrival, respectively. The steering vectors are given by

$$\mathbf{a}_t(\phi_{t,l}) = \frac{1}{\sqrt{N_t}} [a_{t,1}(\phi_{t,l}), \ldots, a_{t,N_t}(\phi_{t,l})] \tag{11}$$

$$\mathbf{a}_r(\phi_{r,l}) = \frac{1}{\sqrt{N_r}} [a_{r,1}(\phi_{r,l}), \ldots, a_{r,N_r}(\phi_{r,l})] \tag{12}$$

The elements of transmit and receive steering vectors are given by

$$a_{t,i}(\phi_{t,l}) = e^{-j\omega\tau_{i,t,l}} = e^{-j2\pi(i-1)\frac{d_t}{\lambda}\sin(\phi_{t,l})}, \quad i = 1, 2, \ldots, N_t \tag{13}$$

$$a_{r,i}(\phi_{r,l}) = e^{-j\omega\tau_{i,r,l}} = e^{-j2\pi(i-1)\frac{d_r}{\lambda}\sin(\phi_{r,l})}, \quad i = 1, 2, \ldots, N_r \tag{14}$$

where λ is the wavelength, $\omega = \frac{2\pi}{\lambda}$, τ_i is the beamforming delay, and d_t and d_r are the antenna spacing at the eNB and UE, respectively.

III. PROBLEM FORMULATION

In this section we define our optimization problem. Our objective is to maximize the cell user fairness-aware spectral efficiency through joint resource allocation and hybrid beamforming.

The spectral efficiency $(bits/s/Hz)$ of the UE k on the subchannel i is given by

$$R_{k,i} = \log_2(1 + \frac{\gamma_{k,i}}{\Gamma}), \tag{15}$$

where Γ is the SNR gap between Shannon capacity and the performance obtained by the employed modulation and coding scheme in practical wireless channel. For M-QAM modulation and target bit error rate of Pe, $\Gamma = -(2/3)ln(5Pe)$ [22].

The received signal-to-interference-and-noise ratio (SINR) $\gamma_{k,i}$ at the UE k on the subchannel i is given as

$$\gamma_{k,i} = \frac{|\mathbf{h}_{k,i} \mathbf{F}^{AB} \mathbf{f}_{k,i}^{DB}|^2}{\sum_{j \neq k} |\mathbf{h}_{k,i} \mathbf{F}^{AB} \mathbf{f}_{j,i}^{DB}|^2 + \sigma^2} \tag{16}$$

where $\mathbb{E}\left[||\mathbf{h}_{k,i}||_F^2\right] = \frac{N_t N_r}{\rho_{k,i}}$ with $\rho_{k,i} = P_{t,k,i}/P_{r,k,i}$. The overall precoding vector $\mathbf{f}_{k,i}^{\mathcal{B}} = \mathbf{F}^{AB}\mathbf{f}_{k,i}^{DB}$ provides the power constraint as $\mathbb{E}\left[||\mathbf{f}_{k,i}^{\mathcal{B}}||_F^2\right] = \frac{1}{N_t N_r}$ such that the average received power at UE k on subchannel i is given by

$$\mathbb{E}\left[||\mathbf{h}_{k,i}||_F^2\right]\mathbb{E}\left[||\mathbf{f}_{k,i}^{\mathcal{B}}||_F^2\right] = \frac{1}{\rho_{k,i}} \tag{17}$$

This average received power is obtained through $P_{r,k,i} = \frac{P_{t,k,i}}{\rho_{k,i}}$, where $P_{t,k,i}$ is the transmit power allocated to the symbol of UE k on subchannel i.

The well known Proportional Fair (PF) algorithm aims to maximize the logarithmic utility function $\sum_k \log \bar{R}_k$, where $\bar{R}_k$ is the long-term data rate of the user k. This objective is known as proportional fair criteria. This is equivalent to maximize the $\sum_k R_k(t)/\bar{R}_k$ where $R_k(t)$ is total data transmitted to user k at time t [23], [24]. In order to achieve balance tradeoff between throughput and fairness, we use PF based spectral efficiency maximization. We define per user proportional fairness metric as

$$U(\mathbf{f}_{k,i}^{\mathcal{B}}) = \frac{R_{k,i}(t)}{\bar{R}_{k,i}(t)}, \forall i, k, \tag{18}$$

where $\bar{R}_{k,i}(t)$ is average spectral efficiency (moving average) over a past window of length $T_w = 1/\alpha$ [25], as

$$\bar{R}_{k,i}(t) = \alpha R_{k,i}(t-1) + (1-\alpha)\bar{R}_{k,i}(t-1), \tag{19}$$

We consider the system that can select the subsets of UEs on different subchannels to maximize the utility function. For K number of UEs in the system the eNB can select from 1 to K_i UEs on subchannel i. Then, there are a total of 2^K possible UEs combinations on subchannel i. Since the possible independent spatial layers are upper bounded by $\min(N_t, N_r)$ and we assume $N_r < N_t$, therefore $\varphi_{i,l} \subseteq \{1, 2, \ldots, K\}$ for $l = 1, 2, \ldots, 2^K$ denotes the l^{th} UE assignment set on subchannel i, containing the indices of a set of UEs.

The spectral efficiency of UE k on subchannel i is given by

$$R_{k,i} = \chi_{i,l}\log_2(1 + \frac{\gamma_{k,i}}{\Gamma}), \tag{20}$$

where $\chi_{i,l} \in \{0, 1\}$ is a binary decision variable such that it is equal to one if an UE combination l is selected on subchannel i, otherwise it is equal to zero. Now we formulate our optimization problem for joint resource allocation and precoders design with the objective to maximize the utility function as

$$\begin{aligned}
&\max_{\mathbf{f}_{k,i}^{\mathcal{B}}: k\in\varphi_{i,l}} \sum_{i=1}^{N_f}\sum_{l=1}^{2^K}\sum_{k\in\varphi_{i,l}} U\left(\mathbf{f}_{k,i}^{\mathcal{B}}\right) \\
&\text{subject to } C1: \; tr(\mathbf{F}_i^{DB^H}\mathbf{F}^{AB^H}\mathbf{F}^{AB}\mathbf{F}_i^{DB}) \le P_i, \quad \forall i \\
&\qquad C2: \; rank(\mathbf{F}^{AB}\mathbf{F}^{DB}) \le N_{RF}, \\
&\qquad C3: \; \sum_{l\in\mathcal{L}} \chi_{i,l} = 1 \quad \forall i.
\end{aligned} \tag{21}$$

where $\mathcal{L}$ is a set of all possible consecutive 1's from 1 to $2^K - 1$, i,e., $\mathcal{L} = \{2^1 - 1, 2^2 - 1, \ldots, 2^K - 1\}$. To the extent of the authors' knowledge, no general solution to the above optimization problem (21) exists in the literature. In order to make the problem tractable we apply the time sharing techniques of [26] to make the objective function convex. We use the *pseudo user* concept of [27] for each users' assignment set. It has been shown that for systems with large number of subchannels, like in the mmWave frequency band, the time sharing techniques such that the binary decision variable $\chi_{i,l}$ can take any real value between 0 and 1, has zero duality gap [28], [29].

IV. PROPOSED SOLUTION

The multi-users MIMO system in the network provides a number of opportunities, such as spatial multiplexing, transmit or receive diversity gain, multi-user diversity, beamforming. These benefits come with tradeoff among them. In this paper, we present resource allocation algorithm to maximize the PF spectral efficiency under the per subchannel power and the beamforming rank constraints as shown in (21).

A. USERS' CHANNEL DECOUPLING

At each transmission slot, the eNB decides on the subchannel allocation and the transmit beamformers for the downlink. In multi-user massive MIMO transmission more than one UE share a certain subchannel. In this case, zero-forcing (ZF) linear block diagonal technique [30] can be used to spatially separate the UEs which creates decoupled channels for all the UEs. Zero-forcing is a suboptimal but low complexity approach within the linear precoders' class. It performs very well in the high SNR regime or as the multiuser diversity increases, the probability of matching users with spatially compatible channels grows [18], [31], [32]. Moreover, with the introduction of large antenna arrays, such that $N_t \gg N_r$ has shown that zero-forcing beamforming can achieve up to 98% of the non-linear dirty paper coding (DPC) capacity [33]. In order to make this paper self-contained, we describe the block diagonalization briefly. For simplicity, first we consider the downlink transmission over one subchannel i. If there are K_i UEs on subchannel i, then the downlink channel on this subchannel is expressed as $N_r \times N_t$ matrix

$$\mathbf{H}_i = [\mathbf{H}_{1,i}^T, \ldots, \mathbf{H}_{K_i,i}^T]^T \tag{22}$$

For UE j, we define the following $(N_r - n_j) \times N_t$ channel matrix

$$\mathbf{H}'_{j,i} = [\mathbf{H}_{1,i}^T, \ldots, \mathbf{H}_{j-1,i}^T, \mathbf{H}_{j+1,i}^T, \ldots, \mathbf{H}_{K_i,i}^T]^T \tag{23}$$

Let the rank of $\mathbf{H}'_{j,i}$ be denoted by $r'_{j,i}$, then the nullspace of $\mathbf{H}'_{j,i}$ has dimension $N_t - r'_{j,i} \ge n_j$. Performing the SVD of each user's channel matrix on subchannel i leads to the following

$$\mathbf{H}'_{j,i} = \mathbf{U}'_{j,i}\Sigma'_{j,i}\mathbf{V}'^H_{j,i} = \mathbf{U}'_{j,i}\Sigma'_{j,i}[\mathbf{V}'^{(1)}_{j,i}\,\mathbf{V}'^{(0)}_{j,i}]^H, \tag{24}$$

where $\mathbf{U}'_{j,i}$ and $\mathbf{V}'_{j,i}$ are the unitary matrices. The columns of $\mathbf{U}'_{j,i}$ are the left singular vectors of $\mathbf{H}'_{j,i}$, the columns of $\mathbf{V}'_{j,i}$ are the right singular vectors of $\mathbf{H}'_{j,i}$, and $\Sigma'_{j,i}$ is a diagonal matrix in which the diagonal entries are the singular values of $\mathbf{H}'_{j,i}$. In the last equality of (24), $\mathbf{V}'^{(1)}_{j,i}$ holds the first $r'_{j,i}$

right singular vectors of $\mathbf{H}'_{j,i}$ and $\mathbf{V}'^{(0)}_{j,i}$ contains the $N_t - r'_{j,i}$ singular vectors of $\mathbf{H}'_{j,i}$ which are in the nullspace of $\mathbf{H}'_{j,i}$. The columns of $\mathbf{V}'^{(0)}_{j,i}$ are best suited for UE j beamforming vector $\mathbf{f}^B_{j,i}$ because they will provide zero interference at other UEs. Usually $\mathbf{V}'^{(0)}_{j,i}$ contains more number of columns than the n_j, therefore we use some linear combinations of the columns of $\mathbf{V}'^{(0)}_{j,i}$ to make at most n_j columns.

$$\mathbf{H}_{j,i}\mathbf{V}'^{(0)}_{j,i} = \mathbf{U}_{j,i}\begin{bmatrix}\mathbf{\Sigma}_{j,i} & \mathbf{0}\\ \mathbf{0} & \mathbf{0}\end{bmatrix}\begin{bmatrix}\mathbf{V}^{(1)}_{j,i} & \mathbf{V}^{(0)}_{j,i}\end{bmatrix}, \tag{25}$$

where $\mathbf{H}_{j,i}\mathbf{V}'^{(0)}_{j,i}$ gives the matrix with columns as the linear combinations of the columns of $\mathbf{V}'^{(0)}_{j,i}$. The right hand side of the equation is the SVD of $\mathbf{H}_{j,i}\mathbf{V}'^{(0)}_{j,i}$, where $\mathbf{\Sigma}_{j,i}$ is $r_{j,i} \times r_{j,i}$ diagonal matrix and $\mathbf{V}^{(1)}_{j,i}$ represents the $r_{j,i}$ singular vectors with nonzero singular values of $\mathbf{H}_{j,i}\mathbf{V}'^{(0)}_{j,i}$. The transmit beamforming matrix $\mathbf{f}^B_{j,i} = \mathbf{H}_{j,i}\mathbf{V}'^{(0)}_{j,i}$ maximizes the UE j spectral efficiency without any inter-UE interference. The transmit beamforming matrix for subchannel i is defined as

$$\mathbf{F}^B_i = [\mathbf{f}^B_{1,i}, \ldots, \mathbf{f}^B_{K_i,i}]\mathbf{P}^{1/2}_i, \tag{26}$$

where $\mathbf{f}^{B\,H}_{j,i}\mathbf{f}^B_{j,i} = \mathbf{I}, \quad 1 \le j \le K_i$ and $\mathbf{P}_i$ is a block diagonal matrix whose elements scale the power allocated to each interference-free virtual subchannel for all UEs. For a particular UE some virtual spatial subchannels may not be used which is indicated by the zero values of the diagonal elements of $\mathbf{P}_{k,i}$ matrix. The pre-processed received signal at UE k on subchannel i is given by

$$\begin{aligned}\tilde{\mathbf{y}}_{k,i} &= \mathbf{H}_{k,i}\mathbf{x}_{k,i} + \mathbf{w}_{k,i}\\ &= \mathbf{H}_{k,i}\mathbf{f}^B_{k,i}\mathbf{P}^{1/2}_{k,i}\mathbf{s}_{k,i} + \mathbf{w}_{k,i}\\ &= \Sigma_{k,i}\mathbf{P}^{1/2}_{k,i}\mathbf{s}_{k,i} + \mathbf{w}_{k,i}\end{aligned} \tag{27}$$

It can be seen that the data streams for each UE are decoupled. The UE k spectral efficiency on subchannel i under block diagonal constraint is given by

$$R_{k,i} = \chi_{i,l}\log_2\left|\mathbf{I} + \frac{\Sigma^2_{k,i}\mathbf{P}_{k,i}}{\Gamma}\right| \tag{28}$$

B. PROPORTIONAL FAIRNESS HYBRID BEAMFORMING

The proposed user scheduling and subchannel allocation algorithm is based on [5], with the aim to maximize the PF spectral efficiency subjected to the per subchannel power and transmit beamforming matrix rank constraints as given in (21). There is no general solution to the problem in (21). The PFHB algorithm maximizes the PF spectral efficiency for a fixed power per subchannel and a given rank constraint. We express the PFHB precoding matrix as a product of analog and digital beamforming matrices ($\mathbf{F}^B_i = \mathbf{F}^{AB}_{(N_t\times N_{RF})}\mathbf{F}^{DB}_{i,(N_{RF}\times K)}$). First we obtain the user set for each subchannel that maximizes the PF spectral efficiency. The non-selected users give zero column vector in the precoding matrix for each subchannel. For the selected users per subchannel, we form a combined block diagonal zero-forcing precoding matrix which is known as practical, low complexity, near optimal precoding [15], [34]. Then, the $N_t \times N_{RF}$ analog matrix $\mathbf{F}^{AB}$ is obtained by selecting N_{RF} dominant left singular vectors of $SVD(\mathbf{F}^B)$. Finally, for fixed $\mathbf{F}^{AB}$, we find $\mathbf{F}^{DB}_i$ for each subchannel that maximizes the PF utility. The operation of the PFHB algorithm is as follows:

Given the input parameters in line 1 of Algorithm 1 it starts with initialization phase having two sets: an empty set of UEs $\mathcal{K}_i$ on subchannel i and a set of UEs to be scheduled $\mathcal{K}_t$. In MU-MIMO OFDM systems, when $N_t > \sum_{k=1}^{K} n_k$, each subchannel i can be spatially allocated to various UEs. For each subchannel i, the inner *while* loop (line 21) runs for K_i times. Each time, the sum of the utility function with UEs in set $\mathcal{K}_i$ plus the utility function of each UE $k' \in \mathcal{K}_t$ is evaluated in line 10. Line 11 selects k'^* which maximizes the utility function. Update the $\mathbf{F}^B_i$ and $U(\mathbf{F}^B_i)^{updated}$. If $U(\mathbf{F}^B_i)^{updated}$ is greater than or equal to the last $U(\mathbf{F}^B_i)^{last}$ then the selected UE k'^* is added in the set $\mathcal{K}_i$ and removed from the set $\mathcal{K}_t$. Store the updated values of $U(\mathbf{F}^B_i)^{updated}$ and $U(\mathbf{F}^B_i)^{last}$ and repeat the loop for $k = 2, 3, \ldots, K_t$. On the exit of *while* loop (8-24) we will have the UEs in the set $\mathcal{K}_i$ that maximizes the utility function in (21). After finishing for all subchannels, the overall transmit beamforming matrix $\mathbf{F}^B$ is formed by horizontal concatenation of all $\mathbf{F}^B_i$ ($i = \{1, 2, \ldots, N_f\}$). In line 26, $\mathbf{F}^B$ is checked for the rank constraint; if it is less than or equal to N_{RF} then $\mathbf{F}^{AB}$ and $\mathbf{F}^{DB}_i$ are obtained from the *QR*-decomposition of $\mathbf{F}^B$. But if the rank constraint is not satisfied, then arrange the $\mathbf{F}^B_i$ in descending order and take the first i_{min} number of $\mathbf{F}^B_i$ that gives $rank(\mathbf{F}^B) \ge N_{RF}$. The analog beamforming matrix $\mathbf{F}^{AB}$ is obtained through the first N_{RF} number of left singular vectors of $\mathbf{F}^B$ as shown in lines 34 and 35. To find the digital beamforming matrix $\mathbf{F}^{DB}$, repeat the algorithm from line 8 to 28 by using updated channel matrix $\tilde{\mathbf{H}}_i = \mathbf{H}_{i\,(N_r\times N_t)}\mathbf{F}^{AB}_{(N_t\times N_{RF})}$.

C. OPTIMAL SOLUTION USING SEMIDEFINITE PROGRAMMING

In this subsection, we transform our problem to the form of convex optimization problem where we can use the standard semidefinite programming (SDP) techniques to get the optimal solution for the relaxed problem. In the optimization problems with convex objective functions and constraints except the non-convex rank constraint, it is generally desired to keep the rank of matrix smaller than a given value. For these problems, the nuclear norm often serves as a convex substitute for the rank because it is the convex envelop of the rank [35]. Our optimization problem in (21) with nuclear norm penalty becomes

$$\begin{aligned}\min_{\xi,\mathbf{f}^B_{k,i}:k\in\varphi_{i,l}} \quad & -\sum_{i=1}^{N_f}\sum_{l=1}^{2^K}\sum_{k\in\varphi_{i,l}} U\left(\mathbf{f}^B_{k,i}\right) + \xi\|\mathbf{F}\|_*\\ \text{subject to } C1:\ & tr(\mathbf{F}^{DB\,H}_i\mathbf{F}^{AB\,H}\mathbf{F}^{AB}\mathbf{F}^{DB}_i) \le P_i, \quad \forall i\\ C2:\ & rank(\mathbf{F}^{AB}\mathbf{F}^{DB}) \le N_{RF}\\ C3:\ & \sum_{l=1}^{2^K}\chi_{i,l} \le 1, \quad \forall i\\ C4:\ & \mathbf{F} \succeq 0,\end{aligned} \tag{29}$$

Algorithm 1 PFHB Resource Allocation Algorithm

Inputs
K_t: Number of UEs to be scheduled
N_f: Number of subchannels
K_i: Number of UEs to be scheduled on subchannel i
N_{RF}: Number of RF chains
Initialization
$\mathcal{K}_t = \{1, \ldots, K_t\}$, $U(\mathbf{F}_i^B)^{last} = 0$, $\mathcal{K}_i = \{\}$, $\forall i$
{Resource allocation to maximize the PF spectral efficiency}
while $i \leq N_f$ **do**
  while $k \leq K_t$ **do**
    Compute $U(\mathbf{F}_i^B) = U(\mathbf{F}_i^B) + U(\mathbf{f}_{k',i}^B), \quad \forall k' \in \mathcal{K}_t$
    $k'^* = \arg\max_{k'} \{U(\mathbf{F}_i^B)\}$
    Update $\mathbf{F}_i^B$ and $U(\mathbf{F}_i^B)^{update}$ with UE k'^*
    if $U(\mathbf{F}_i^B)^{updated} \geq U(\mathbf{F}_i^B)^{last}$ **then**
      $\mathcal{K}_i = \mathcal{K}_i \cup \{k'^*\}$
      $\mathcal{K}_t = \mathcal{K}_t - \{k'^*\}$
      $U(\mathbf{F}_i^B)^{last} = U(\mathbf{F}_i^B)^{updated}$
      $k++$
    else
      break
    end if
  end while
  $\chi_{i,l} = 1$
  $i++$
end while
Stack the beamforming matrices $\mathbf{F}^B = [\mathbf{F}_1^B, \ldots, \mathbf{F}_{N_f}^B]$
if $rank(\mathbf{F}^B) \leq N_{RF}$ **then**
  $(\mathbf{F}^{AB}, \mathbf{F}_i^{DB}) = QRdecomposition(\mathbf{F}_i^B)$
  End of Algorithm
else
  $U(\mathbf{F}^B)^{ordered} = sort(U(\mathbf{F}_i^B), descending)$
  while $i \leq length(U(\mathbf{F}_i^B)^{ordered})$ **do**
    $\mathbf{F}^B = horizontalStack(F_i^B)$
    if $rank(\mathbf{F}^B) \geq N_{RF}$ **then**
      $SVD(\mathbf{F}^B) = \mathbf{U}\Sigma\mathbf{V}^H$
      $\mathbf{F}^{AB} = \mathbf{U}(:, 1 : N_{RF})$
      break
    end if
    $i++$
  end while
end if
Repeat line 8 to 28
Output
$\mathbf{F}^B = [\mathbf{F}_1^B, \ldots, \mathbf{F}_{N_f}^B]$
$[\mathcal{K}_1, \ldots, \mathcal{K}_{N_f}]$

where $\mathbf{F} = \mathbf{F}^B\mathbf{F}^{BH}$ and the parameter $\xi \geq 0$. We replace the rank constraint by convex inequality constraint to force the rank to be at most the desired value. The following lemma replaces the rank constraint by convex constraint that ensures the desired upper limit on rank for any nonzero matrix $\mathbf{F}$.

Lemma 1: Given integer q with $N_t/2 < q < N_t$. Let $\mathbf{F} = \mathbf{F}^B\mathbf{F}^{BH}$, which is an $N_t \times N_t$ symmetric semidefinite matrix, satisfies $r\|\mathbf{F}\|_2 - tr(\mathbf{F}) \geq 0$, where $q-1 < r \leq q$, then either $rank(\mathbf{F}) \leq q$, or $\mathbf{F} = \mathbf{0}$.

Proof: If $\mathbf{F} = 0$, the constraint is already satisfied. Consider the case when $\mathbf{F} \neq 0$. Assume $\sigma_1 \geq \sigma_2 \geq \ldots \geq \sigma_{N_t} \geq 0$ be the ordered singular values of $\mathbf{F}$. Using the definitions of the matrix induced 2-norm and trace [35], the constraint can then be written as $r\sigma_1 - \sum_{i=1}^{N_t} \sigma_i \geq 0$, and it follows that:

$$r\sigma_1 - \sum_{i=q+1}^{N_t} \sigma_i \geq \sum_{j=1}^{q} \sigma_j$$

$$r\sigma_1 - (N_t - q)\sigma_1 + (N_t - q)\sigma_1 - \sum_{i=q+1}^{N_t} \sigma_i \geq \sum_{j=1}^{q} \sigma_j$$

$$(r - N_t + q)\sigma_1 + \sum_{i=q+1}^{N_t} (\sigma_1 - \sigma_i) \geq q\sigma_q$$

Both terms on left hand side of the last inequality are positive, therefore left hand side is strictly positive, which then requires permissible values of σ_1 to σ_q, and thus $rank(\mathbf{F}) \leq q$. ■

This constraint in (29) yields convex optimization problem in standard form as

$$\begin{aligned} \min_{\xi, \mathbf{f}_{k,i}^B : k \in \varphi_{i,l}} \quad & -\sum_{i=1}^{N_f} \sum_{l=1}^{2^K} \sum_{k \in \varphi_{i,l}} U\left(\mathbf{f}_{k,i}^B\right) + \xi \|\mathbf{F}\|_* \\ \text{subject to } C1: \quad & tr(\mathbf{F}_i^{DBH}\mathbf{F}^{ABH}\mathbf{F}^{AB}\mathbf{F}_i^{DB}) \leq P_i, \quad \forall i \\ C2: \quad & r\|\mathbf{F}\|_2 - tr(\mathbf{F}) \geq 0 \\ C3: \quad & \sum_{l=1}^{2^K} \chi_{i,l} \leq 1, \quad \forall i \\ C4: \quad & \mathbf{F} \succeq 0, \end{aligned} \tag{30}$$

This is a convex semidefinite programming (SDP) problem which can be solved by the standard SDP techniques. Before applying the SDP technique we need to find the optimal value of parameter ξ. It can be obtained by first finding the dual of problem (30) and then minimizing over the Lagrangian as shown in [36]. If the constraint $C2$ individually holds for all subchannels, then, the optimization problem can be transformed to subchannel level which reduces the computational complexity from $\mathcal{O}(2^{N_f K})$ to $\mathcal{O}(N_f 2^K)$. Subchannel level $C2$ is not tractable, therefore, we split the problem into two subproblems and solve in next section.

D. PROPORTIONAL FAIRNESS RELAXED OPTIMIZATION (PFRO): A SUBOPTIMAL SOLUTION

We propose a subchannel level two step heuristic algorithm PFRO; inspired by the optimization problem in (30). We relaxed the objective function in (30) by removing $\xi\|\mathbf{F}\|_*$. It has been shown [36] that for better performance, the value of the parameter ξ should be positive and close to zero, so that, we can safely transform the objective function in (30) to

one in (31). The constraint $C1$ is simply limits the subchannel level power allocation to each user within the available power per subchannel. The transformed rank constraint in $C2$ is realized by Eckart-Young theorem [37] of low rank approximation in the second step of algorithm. In constraint $C3$, the relaxation on $\chi_{i,l}$ has been removed and $\chi_{i,l}$ becomes a binary variable. The resultant mixed integer optimization problem is not convex because of the integer constraint. The global optimal of such a mixed integer optimization problem requires the combination of conventional convex optimization algorithm with an exhaustive search.

In the first step, we solve the following convex optimization problem by first converting (see Appendix A) it into a mixed integer disciplined convex programming (MIDCP) and then using CVX [38] with MOSEK solver [39].

$$\begin{aligned} \max_{p_{k,i},\chi_{i,l}} \quad & \sum_{l=1}^{2^K} \sum_{k\in\varphi_{i,l}} U(\mathbf{f}_{k,i}^{B}) \\ \text{subject to } C1\text{:} \quad & \sum_{k=1}^{K} p_{k,i} \le P_i, \quad \forall i \\ C2\text{:} \quad & \sum_{l=1}^{2^K} \chi_{i,l} = 1, \quad \forall i \\ C3\text{:} \quad & p_{k,i} \ge 0, \quad \forall k, i. \end{aligned} \tag{31}$$

where $\chi_{i,l}$ and $p_{k,i}$ are the optimization variables. The output $\chi_{i,l}^{*}$ provides the optimal users' combination l on the subchannel i, and $p_{k,i}$ allocates the subchannel power P_i among the selected users to maximize the PF spectral efficiency.

In line 13, we determine the precoding vector for UE k on subchannel i with the help of the binary selection variable $\chi_{i,l}^{*}$. The binary variable $\chi_{i,l}^{*}$ corresponds to the optimal users' set φ_{i,l^*}. In binary form l^* can be written as $l^* = [l_1^*, \ldots l_K^*]$ where the binary digit $l_k^* = 1$ if the user k is in the selected users' set φ_{i,l^*}. Then, the precoder of UE k on subchannel i is given by

$$\mathbf{f}_{k,i}^{B*} = \begin{cases} \mathbf{f}_{k,i}^{B} & \text{for } l_k^* = 1, \\ 0 & \text{for } l_k^* = 0. \end{cases} \tag{32}$$

The precoding matrix for subchannel i is calculated in line 14. In line 15, 16, the average spectral efficiency has been calculated for the input of *cvxOptimization* function in the next iteration.

In the second step, the overall precoding matrix $\mathbf{F}^{B*}$ is obtained by stacking the precoding matrices of all subchannels in line 19. The rank of $\mathbf{F}^{B*}$ is checked against the input N_{RF}. If it is greater than N_{RF}, then, low rank approximation [37] is used to ensure the rank constraint. Finally, the analog and digital beamforming matrices are obtained from QR-decomposition as shown in lines 21 to 23.

In practical implementations, the digital beamforming can be realized at the baseband frequency whereas, the analog beamforming can be implemented by using low cost phase shifters (PSs) at the RF frequency. In order to realize the analog beamforming with analog phase shifters, we need a constant magnitude beamforming matrix. This can be obtained from following *lemma*:

Lemma 2: For a matrix $\mathbf{A} \in \mathbb{C}^{m\times n}$, *any element* $\mathbf{a}_{mn}$ *can be represented by the sum of two unit magnitude vectors, given that* $-2a_{max} \le a_{mn} \le 2a_{max}$, *where* $a_{max} = \max_{m,n}\{a_{mn}\}$.

Proof: The complex matrix element can be written as

$$\mathbf{a}_{mn} = \frac{a_{mn}}{2a_{max}} e^{j\phi_{mn}} \tag{33}$$

since $-2a_{max} \le a_{mn} \le 2a_{max}$, we can have

$$\cos\theta_{mn} = \frac{a_{mn}}{2a_{max}} \tag{34}$$

using Euler identity,

$$\cos\theta_{mn} = \frac{e^{j\theta_{mn}} + e^{-j\theta_{mn}}}{2} \tag{35}$$

comparing (34) and (35) and then substituting $\frac{a_{mn}}{2a_{max}}$ in (33), we get

$$\mathbf{a}_{mn} = \frac{1}{2}\left(e^{j(\phi_{mn}+\cos^{-1}(\frac{a_{mn}}{2a_{max}}))} + e^{j(\phi_{mn}-\cos^{-1}(\frac{a_{mn}}{2a_{max}}))}\right) \tag{36}$$

■

Lemma 2 enables the practical implementation of the evaluated analog beamforming matrices in Algorithms 1 and 2.

E. COMPLEXITY ANALYSIS

In this subsection, we provide the complexity analysis of Algorithms 1 and 2. The complexity of the exhaustive search algorithm for the solution of the optimal hybrid beamforming with PF in (21) even after the users' channel decoupling in subsection IV-A is $\mathcal{O}(2^{KN_f})$. Before going inside of algorithms complexity we explain the complexities of some commonly used mathematical operations. The complexity of SVD, rank, QR decomposition and pseudo-inverse of a matrix of dimension $m \times n$ is $\mathcal{O}(\min(mn^2, m^2n))$, and for a matrix multiplication of matrices of dimensions $m \times n$ and $n \times p$ is $\mathcal{O}(mnp)$ [40]. From Algorithm 1, we can observe that the complexity of PFHB comes from the following parts:

From line 8-22, there are two nested *while* loops, i.e., N_f loop and K loop. With K loop we calculate the utility function U, therefore, the complexity is $\mathcal{O}(N_t N_f K)$. Line 26 contains the rank of matrix $\mathbf{F}^B$ with complexity $\mathcal{O}(N_t^2 K N_f)$ (assuming $KN_f > N_t$). Line 27 is subchannel-wise QR decomposition therefore it has the complexity $\mathcal{O}(K^2 N_t)$. Line 30 contains subchannel-wise sorting of the utility function with complexity $\mathcal{O}(N_f \log N_f)$. Finally, lines 33-34 give rank and SVD with complexity $\mathcal{O}(\min(N_t(Ki)^2, N_t^2 Ki))$ where i is the number of subchannels that gives $rank(\mathbf{F}^B) \approx N_{RF}$. Using the rules of constant factors, polynomials, and exponential big-oh expressions [41, Ch. 3], we sum up the overall complexity of the PFHB algorithm as $\mathcal{O}(N_t^2 K N_f)$.

In Algorithm 2 the complexity contributing factors are:

lines 8-11 contain channel matrix, zero forcing beamforming matrix (pseudoinverse), and CNR with complexity $\mathcal{O}(N_t)$. In line 12, we use CVX for subchannel level optimal solution

Algorithm 2 PF Relaxed Optimization (PFRO) Resource Allocation Algorithm

1: **Inputs**
2: K: Number of UEs to be scheduled
3: N_f: Number of subchannels
4: K_i: Number of UEs to be scheduled on subchannel i
5: N_{RF}: Number of RF chains
6: *Initialization*
7: $\mathcal{K} = \{1, \ldots, K\}$, $\mathcal{K}_i = \{\}$, $\forall i$
{**Step 1**:Resource allocation to maximize the PF spectral efficiency}
8: **while** $i \leq N_f$ **do**
9: Compute $\mathbf{H}_i$ using (10)
10: Compute zero forcing beamforming matrix $\mathbf{F}_i^B$
11: Compute carrier-to-noise ratio CNR_i
12: Compute $[\chi_{i,l}^*, p_{k,i}^*] = cvxOptimization(P_i, K, CNR_i, \bar{R}_i(t))$ (see Appendix A)
13: Compute $\mathbf{f}_{k,i}^{B*}$ using (32)
14: $\mathbf{F}_i^{B*} = [\mathbf{f}_{1,i}^{B*}, \ldots, \mathbf{f}_{K,i}^{B*}]$
15: Compute spectral efficiency $R_i(t) = \log_2(1+p_i^* CNR_i)$
16: Update average spectral efficiency $\bar{R}_i(t) = \alpha R_i(t-1) + (1-\alpha)\bar{R}_i(t-1)$
17: $i++$
18: **end while**
{**Step 2**: Rank constraint realization}
19: Stack the beamforming matrices $\mathbf{F}^{B*} = [\mathbf{F}_1^{B*}, \ldots, \mathbf{F}_{N_f}^{B*}]$
20: **if** $rank(\mathbf{F}^{B*}) \leq N_{RF}$ **then**
21: $(\mathbf{F}^{AB*}, \mathbf{F}^{DB*}) = QRdecomposition(\mathbf{F}^{B*})$
22: $\mathbf{F}^{AB*} = \mathbf{F}^{AB*}(:, 1 : N_{RF}), \rightarrow \mathbf{F}^{AB*} \in \mathbb{C}^{N_t \times N_{RF}}$
23: $\mathbf{F}^{DB*} = \mathbf{F}^{DB*}(1 : N_{RF}, :), \rightarrow \mathbf{F}^{DB*} \in \mathbb{C}^{N_{RF} \times (N_f \times K)}$
24: End of Algorithm
25: **else**
26: $SVD(\mathbf{F}^{B*}) = \mathbf{U}\Sigma\mathbf{V}^H$
27: $\tilde{\Sigma} = diag(\sigma_1, \ldots, \sigma_{N_{RF}}, 0, ...0)$
28: $\mathbf{F}^{B*} = U\tilde{\Sigma}V$
29: go to line 21
30: **end if**

that has the worse-case complexity $\mathcal{O}(N_f 2^K)$ (with exhaustive search method). Lines 13-18 have $\mathcal{O}(1)$ except line 15 which has complexity $\mathcal{O}(\log K)$. Line 20, 21, and 26 contain rank, QR decomposition, and SVD, respectively, for those the complexity is $\mathcal{O}(N_t^2 K N_f)$. To sum up, the overall complexity of the PFRO algorithm is $\mathcal{O}(N_f 2^K)$.

In summary, the sub-optimal PF-based hybrid beamforming algorithm PFHB has the lowest complexity $\mathcal{O}(N_t^2 K N_f)$, whereas, the relaxed optimal algorithm PFRO shows a significant performance improvement at the cost of exponential complexity in K, as $\mathcal{O}(N_f 2^K)$.

V. SIMULATION RESULTS

In the simulation setup, number of subchannels N_f is 64 and independent Rayleigh distributed complex random variables $\mathcal{CN}\{0, 1\}$ are generated for channel coefficients. The transmit antenna array is ULA with antenna spacing $d = \lambda/2$. Channel matrix is generated by using (10). We assume infinite resolution PS. It should be noted that the MTDB and PFDB graphs in the simulation results are to show the performance of an ideal non-feasible fully digital precoder as a reference. Simulations are averaged over 100 channel realizations for each subchannel.

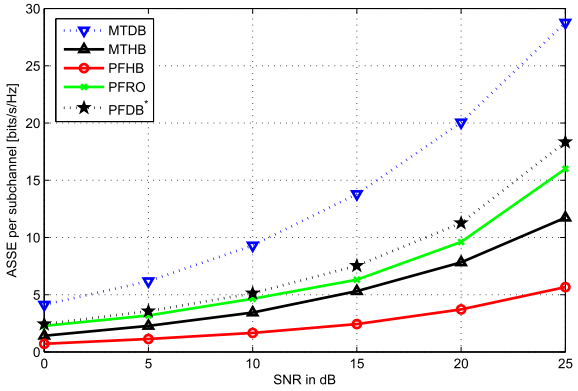

FIGURE 2. Average sum spectral efficiency per subchannel.

A. SUM SPECTRAL EFFICIENCY

Fig. 2, system level average sum spectral efficiency (ASSE) per subchannel is shown. The SNR is varied from 0 to 25dB, where $SNR = \frac{N_f P_i}{K_t \sigma^2}$. The number of users K_t is 8, noise power density is $-174dBm/Hz$, and the subchannel bandwidth is $5MHz$. Since the complex channel coefficients are i.i.d Rayleigh distributed with zero mean and variance 1, and zero forcing precoding is employed with $\rho_{k,i} = 1$, $\forall k, i$. It can be seen that at low SNR values all HB schemes are close to each other. The proposed PFHB algorithm gives lower sum spectral efficiency as compared to the MTHB of [18]. The relaxed suboptimal solution PFRO shows the superiority over the MTHB of [18] and proposed PFHB because PFRO algorithm uses optimal users' combination and optimal power allocation per subchannel.

Fig. 2 also shows that the proposed PFRO scheme is near-optimal, since the sum spectral efficiency gap is less than $2.33bps/Hz$ for all SNR values $0 - 25dB$ and the required SNR gap between the optimal PFDB and the proposed PFRO to achieve the same sum spectral efficiency is within $2dB$, where PFDB is obtained from Algorithm 1 by setting $N_{RF} = N_t$.

B. INDIVIDUAL USER SPECTRAL EFFICIENCY

In practical scenarios, users are at the different distances from the eNB and have different average received SNRs. Fig. 3 shows the individual spectral efficiency when users are placed at gradually increasing distances from the eNB. The transmit power is fixed at $45dBm$. The maximum throughput based MTDB and MTHB give high spectral efficiency to closer users but the edge users suffer from the low or zero value,

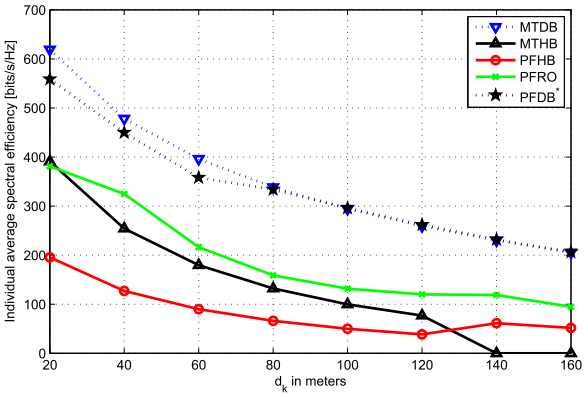

FIGURE 3. **Individual spectral efficiency when $K_t = 8$ users are placed at different distances from eNB.**

whereas, the PF-based PFDB, PFRO and PFHB try to achieve the best tradeoff between spectral-efficiency and fairness. The PFDB individual spectral efficiency even reaches the MTDB for some users but sum spectral efficiency is always less than the MTDB. The PFRO provides higher individual user spectral efficiency than PFHB and more uniform spectral efficiency distribution to the users with different distances (average received SNR) as compared to the MTDB and MTHB schemes. The PFDB has best tradeoff between throughput and fairness but at the cost of large number of RF chains and power consumption.

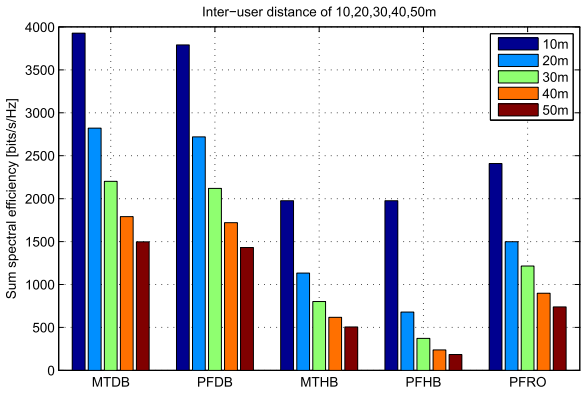

FIGURE 4. **Spectral efficiency comparison of schemes with various inter-user distances.**

Fig. 4 shows the sum spectral efficiency of different schemes with various inter-users distances and coverage areas. For example, with inter-users distance of $20m$, each user has a distance of $20m$ with each other, such that the farthest user has a distance of $20 \times K_t$ ($160m$ radius coverage area when $K_t = 8$) from the eNB. The sum spectral efficiency of two ideal schemes (MTDB and PFDB) is high as expected. Among the three practical hybrid beamforming schemes, the PFRO performs better than MTHB and PFHB for all inter-user distances. In PFRO, the sum spectral efficiency for 400m radius coverage area is greater than the sum spectral efficiency of 160m radius coverage area in PFHB.

TABLE 1. **Simulation Parameters**

Parameter	Value
N_t	64
n_k	1, $\forall k$
N_f	64
N_{RF}	16
L_s	2
ρ	1
$K = K_i = K_t$	8
α	0.8
P_i	$45dBm$
Carrier frequency [21]	$38GHz$
Pathloss exponent [21]	2.21
Subchannel bandwidth	$5MHz$
Noise power density	$-174dBm/Hz$

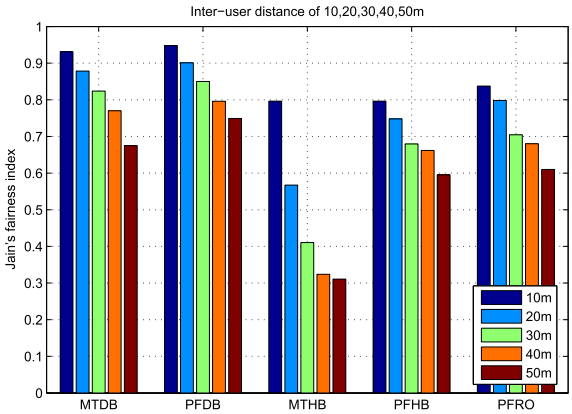

FIGURE 5. **Jain's fairness index.**

C. FAIRNESS

We analyze the performance of the algorithms in terms of fairness using Jain's fairness index [42]. Jains fairness index (JFI) has been widely used as a measure of fairness in communication systems, which is defined as

$$JFI = \frac{\left(\sum_{k=1}^{K} R_k\right)^2}{K \sum_{k=1}^{K} R_k^2} \tag{37}$$

where R_k is the k^{th} users average throughput. As shown in the Fig. 5, PFDB has the highest fairness index among all DB and HB schemes, because of the PF-based resource allocation and the expensive digital beamforming. Among the three HB techniques, the proposed PFRO outperforms the other schemes. Since, the fairness among users depends on the slope of the individual users' throughput, therefore, PFRO and PFHB exhibit approximately the same performance in fairness index as shown in Fig. 5. Again, at very small inter-user distances the PFRO, PFHB and MTHB have same performance but at large inter-user distances, PFRO and PFHB provide high fairness among users.

D. PERFORMANCE OF ALGORITHMS

We analyze the performance of proposed algorithms by calculating the time-elapsed for the sum spectral efficiency

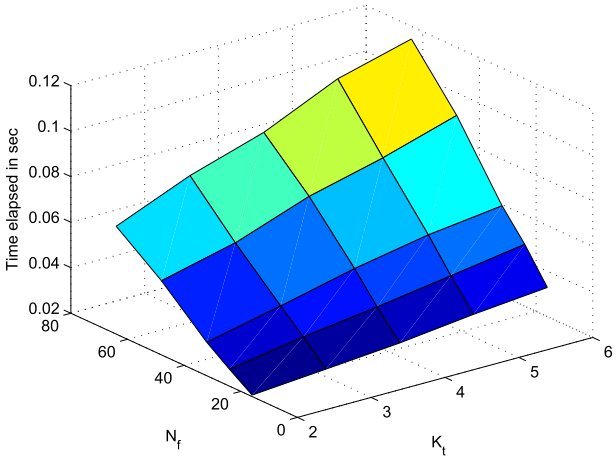

FIGURE 6. Algorithm 1 time elapsed for sum spectral efficiency with different values of K_t and N_f, when average $SNR = 20dB$.

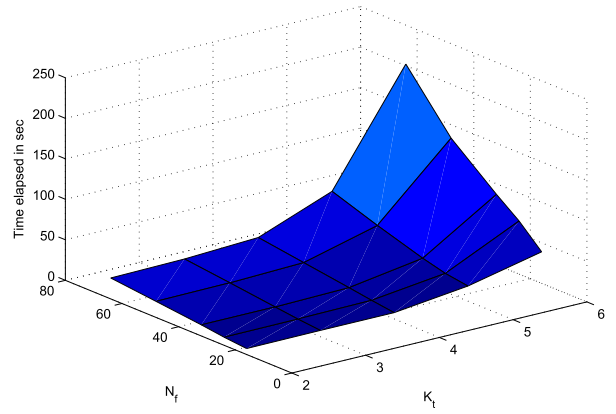

FIGURE 7. Algorithm 2 time elapsed for sum spectral efficiency with different values of K_t and N_f, when average $SNR = 20dB$.

evaluation with different values of the number of users and the number of subchannels in Fig. 6 and Fig. 7. Algorithms 1 and 2 are designed in such a way that ensures their termination in two iterations at the most. In Algorithm 1, $SVD(\mathbf{F}^B)$ in line 34 and the selection of the first N_{RF} left singular columns as analog beamforming matrix in line 35 ensure the algorithm termination in the second iteration. In Algorithm 2, low rank approximation in lines 26, 27, and 28 guarantees the end of algorithm. Within the iteration, the complexity of the algorithms depend on the number of subchannels and the number of users, as discussed in the subsection IV-E. It can be seen in Fig. 6 that the time-elapsed of Algorithm 1 is linear function of the number of users for a fixed number of subchannels and vice versa (linear function of number of subchannels for fixed number of users). This validates the complexity evaluated in the subsection IV-E. Fig. 7 seconds the concluded complexity for Algorithm 2 in subsection IV-E, i.e., the computation time increases linearly with number of subchannels for the fixed number of users, and it increases exponentially with the number of users for the fixed number of subchannels. The comparison of Fig 6 and Fig. 7 reveals the large computation time of the Algorithm 2 as compared to the Algorithm 1. The optimal solution to the problem in (30) has exponential complexity both in number of subchannels and number of users. The proposed solution to the PFRO uses CVX to find the optimal users combination per subchannel and the power allocation for the selected users, and the dominant component of the execution time is due to the *cvxOptimization*() function in line 12 of Algorithm 2.

VI. CONCLUSIONS

In this paper, we present resource allocation algorithms (PFHB and PFRO) to maximize the proportional fairness spectral efficiency under the per subchannel power and the transmit beamforming rank constraints. The PFHB algorithm provides the PF-based hybrid precoding matrix for required number of RF chains. Then, we transform the number of RF chains or rank constrained optimization problem into convex semidefinite programming problem which can be solved by standard techniques. Inspired by the convex SDP problem we present PFRO algorithm. It has been shown that the proposed PFRO scheme provides near-optimal sum spectral efficiency. The performance gap is less than $2.33bps/Hz$ and $2dB$ in terms of sum spectral efficiency and required SNR, respectively, to achieve the same performance. The proposed PFRO provides better performance in sum spectral efficiency, individual spectral efficiency, and fairness index among other HB designs.

APPENDIX A
PROBLEM FORMULATION FOR CVX

CVX is a Matlab-based modeling framework for convex optimization. The user challenging part of CVX is to transform the optimization problem into the disciplined convex programming (DCP). In our transformation, the inputs are the number of users K, carrier-to-noise ratio CNR, per subchannel power P, and the previous average spectral efficiency R_t_1. The outputs are p and X. The utility function in (31) which is defined in (18) contains multiplication of optimization variables which is against the DCP ruleset defined in [38]. In order to express the objective function in CVX format, we use the technique available at [43] to write the spectral efficiency function in line 10 of below code. The sum of logarithmic function is replaced by the geometric function in line 9.

```
1   L=2^K-1;
2   x=de2bi(1:2^K-1,'left-msb');
3   CNRx=CNR_repmat.*x;
4   q_t_1=2.^(R_t_1);

5   cvx_begin
6       cvx_solver mosek
7       variables p(L,K) q(L,K)
8       variable X(L,1) binary
9       maximize(sum(geo_mean(q,2)))
```

```
10        q <= (1 + CNRx .* min(p,P*repmat
          (X,1,K))./q_t_1;
11        p>=zeros(L,K)
12        sum(sum(p,2))<=P
13        sum(X)==1
14    cvx_end
```

REFERENCES

[1] G. Bochechka and V. Tikhvinskiy, "Spectrum occupation and perspectives millimeter band utilization for 5G networks," in *Proc. ITU Kaleidoscope Acad. Conf. Living Converg. World-Impossible Standards*, Saint Petersburg, Russia, 2014, pp. 69–72.

[2] W. Roh *et al.*, "Millimeter-wave beamforming as an enabling technology for 5G cellular communications: Theoretical feasibility and prototype results," *IEEE Commun. Mag.*, vol. 52, no. 2, pp. 106–113, Feb. 2014.

[3] *Part 11: Wireless LAN Medium Access Control (MAC) and Physical Layer (PHY) Specifications Amendment 3: Enhancements for Very High Throughput in the 60 GHz Band*, IEEE Standard 802.11ad, Dec. 2012.

[4] GSMA. *LTE- About Us* . accessed on Oct. 22, 2016. [Online]. Available: http://www.gsma.com/aboutus/gsm-technology/lte

[5] T. E. Bogale, L. B. Le, and A. Haghighat, "User scheduling for massive MIMO OFDMA systems with hybrid analog-digital beamforming," in *Proc. IEEE Int. Conf. Commun.*, London, U.K., Jun. 2015, pp. 1757–1762.

[6] F. Sohrabi and W. Yu, "Hybrid beamforming with finite-resolution phase shifters for large-scale MIMO systems," in *Proc. IEEE 16th Int. Workshop Signal Process. Adv. Wireless Commun.*, Stockholm, Sweden, Jul. 2015, pp. 136–140.

[7] F. Sohrabi and W. Yu, "Hybrid digital and analog beamforming design for large-scale MIMO systems," in *Proc. IEEE Int. Conf. Acoust. Speech Signal Process.*, South Brisbane, QLD, Australia, Apr. 2015, pp. 2929–2933.

[8] R. Méndez-Rial, C. Rusu, A. Alkhateeb, N. González-Prelcic, and R. W. Heath, Jr., "Channel estimation and hybrid combining for mmWave: Phase shifters or switches?" in *Proc. Inf. Theory Appl. Workshop (ITA)*, San Diego, CA, USA, 2015, pp. 90–97.

[9] C. E. Chen, "An iterative hybrid transceiver design algorithm for millimeter wave MIMO systems," *IEEE Wireless Commun. Lett.*, vol. 4, no. 3, pp. 285–288, Jun. 2015.

[10] Z. Xu, S. Han, Z. Pan, and C.-L. I, "Alternating beamforming methods for hybrid analog and digital MIMO transmission," in *Proc. IEEE Int. Conf. Commun.*, London, U.K., Jun. 2015, pp. 1595–1600.

[11] C. Kim, T. Kim, and J. Y. Seol, "Multi-beam transmission diversity with hybrid beamforming for MIMO-OFDM systems," in *Proc. IEEE Globecom Workshop (GC Wkshps)*, Atlanta, GA, USA, Dec. 2013, pp. 61–65.

[12] A. Alkhateeb, O. El Ayach, G. Leus, and R. W. Heath, Jr., "Hybrid precoding for millimeter wave cellular systems with partial channel knowledge," in *Proc. Inf. Theory Appl. Workshop*, San Diego, CA, USA, Feb. 2013, pp. 1–5.

[13] O. El Ayach, R. W. Heath, Jr., S. Abu-Surra, S. Rajagopal, and Z. Pi, "Low complexity precoding for large millimeter wave MIMO systems," in *Proc. IEEE Int. Conf. Commun.*, Ottawa, ON, Canada, Jun. 2012, pp. 3724–3729.

[14] S. Kutty and D. Sen, "Beamforming for millimeter wave communications: An inclusive survey," *IEEE Commun. Surveys Tut.*, vol. 18, no. 2, pp. 949–973, 2nd Quart., 2016.

[15] F. Sohrabi and W. Yu, "Hybrid digital and analog beamforming design for large-scale antenna arrays," *IEEE J. Sel. Topics Signal Process.*, vol. 10, no. 3, pp. 501–513, Apr. 2016.

[16] R. W. Heath, Jr., N. González-Prelcic, S. Rangan, W. Roh, and A. M. Sayeed, "An overview of signal processing techniques for millimeter wave MIMO systems," *IEEE J. Sel. Topics Signal Process.*, vol. 10, no. 3, pp. 436–453, Apr. 2016.

[17] V. Aggarwal, R. Jana, J. Pang, K. K. Ramakrishnan, and N. K. Shankaranarayanan, "Characterizing fairness for 3G wireless networks," in *Proc. IEEE Workshop Local Metropolitan Area Netw.*, Chapel Hill, NC, USA, Oct. 2011, pp. 1–6.

[18] T. Bogale, L. Le, A. Haghighat, and L. Vandendorpe, "On the number of RF chains and phase shifters, and scheduling design with hybrid analog-digital beamforming," *IEEE Trans. Wireless Commun.*, vol. 15, no. 5, pp. 3311–3326, May 2016.

[19] A. Adhikary *et al.*, "Joint spatial division and multiplexing for mm-wave channels," *IEEE J. Sel. Areas Commun.*, vol. 32, no. 6, pp. 1239–1255, May 2014.

[20] O. El Ayach, S. Rajagopal, S. Abu-Surra, Z. Pi, and R. W. Heath, Jr., "Spatially sparse precoding in millimeter wave MIMO systems," *IEEE Trans. Wireless Commun.*, vol. 13, no. 3, pp. 1499–1513, Mar. 2014.

[21] T. S. Rappaport, F. Gutierrez, Jr., E. Ben-Dor, J. N. Murdock, Y. Qiao, and J. I. Tamir, "Broadband millimeter-wave propagation measurements and models using adaptive-beam antennas for outdoor urban cellular communications," *IEEE Trans. Antennas Propag.*, vol. 61, no. 4, pp. 1850–1859, Apr. 2013.

[22] I. Ahmed and A. Mohamed, "Hybrid radio resource allocation and interference coordination for type 1a-relayed long term evolution uplink," *IET Commun.*, vol. 8, no. 11, pp. 1928–1937, Jul. 2014.

[23] M. Andrews, "A survey of scheduling theory in wireless data networks," in *Wireless Communications*. New York, NY, USA: Springer, 2007, pp. 1–17.

[24] S.-B. Lee, I. Pefkianakis, A. Meyerson, S. Xu, and S. Lu, "Proportional fair frequency-domain packet scheduling for 3GPP LTE uplink," in *Proc. IEEE INFOCOM*, Rio de Janeiro, Brazil, Apr. 2009, pp. 2611–2615.

[25] J. Escudero-Garzás, B. Devillers, and A. García-Armada, "Fairness-adaptive goodput-based resource allocation in OFDMA downlink with ARQ," *IEEE Trans. Veh. Technol.*, vol. 63, no. 3, pp. 1178–1192, Mar. 2014.

[26] P. W. C. Chan and R. S. Cheng, "Capacity maximization for zero-forcing MIMO-OFDMA downlink systems with multiuser diversity," *IEEE Trans. Wirel. Commun.*, vol. 6, no. 5, pp. 1880–1889, May 2007.

[27] Y. M. Tsang and R. S. Cheng, "Optimal resource allocation in SDMA/multiinput-single-output/OFDM systems under QoS and power constraints," in *Proc. IEEE Wireless Commun. Netw. Conf.*, vol. 3. Mar. 2004, pp. 1595–1600.

[28] W. Yu, R. Lui, and R. Cendrillon, "Dual optimization methods for multiuser orthogonal frequency division multiplex systems," in *Proc. IEEE Globecom*, Dec. 2004, pp. 225–229.

[29] W. Yu and R. Lui, "Dual methods for nonconvex spectrum optimization of multicarrier systems," *IEEE Trans. Commun.*, vol. 54, no. 7, pp. 1310–1322, Jul. 2006.

[30] Q. Spencer, A. L. Swindlehurst, and M. Haardt, "Zero-forcing methods for downlink spatial multiplexing in multiuser MIMO channels," *IEEE Trans. Signal Process.*, vol. 52, no. 2, pp. 461–471, Feb. 2004.

[31] A. Wiesel, Y. C. Eldar, and S. Shamai, "Zero-forcing precoding and generalized inverses," *IEEE Trans. Signal Process.*, vol. 56, no. 9, pp. 4409–4418, Sep. 2008.

[32] P. V. Amadori, S. Member, C. Masouros, and S. Member, "Low RF-complexity millimeter-wave beamspace-MIMO systems by beam selection," *IEEE Trans. Commun.*, vol. 63, no. 6, pp. 2212–2223, May 2015.

[33] H. Tataria, P. J. Smith, L. J. Greenstein, P. A. Dmochowski, and M. Shafi, "Performance and analysis of downlink multiuser MIMO systems with regularized zero-forcing precoding in Ricean fading channels," in *Proc. IEEE Int. Conf. Commun.*, Kuala Lumpur, Malaysia, May 2016, pp. 1–7.

[34] L. Liang, W. Xu, X. Dong, S. Member, and W. Xu, "Low-complexity hybrid precoding in massive multiuser MIMO systems," *IEEE Wireless Commun. Lett.*, vol. 3, no. 6, pp. 1–5, Dec. 2014.

[35] B. Recht, M. Fazel, and P. A. Parrilo, "Guaranteed minimum-rank solutions of linear matrix equations via nuclear norm minimization," *SIAM Rev.*, vol. 52, no. 3, pp. 471–501, 2010.

[36] V. S. Mai, D. Maity, B. Ramasubramanian, M. C. Rotkowitz, "Convex methods for rank-constrained optimization problems," in *Proc. SIAM Conf. Control Appl.*, 2015, pp. 123–130.

[37] C. Eckart and G. Young, "The approximation of one matrix by another of lower rank," *Psychometrika*, vol. 1, no. 3, pp. 211–218, Sep. 1936.

[38] M. Grant and S. Boyd. (2015). *CVX: MATLAB Software for Disciplined Convex Programming, Version 2.1*. [Online]. Available: http://cvxr.com/cvx

[39] (2016). *Mixed Integer Disciplined Convex Programming (MIDCP) Solver: MOSEK*. [Online]. Available: https://www.mosek.com/

[40] G. H. Golub and C. F. Van Loan, *Matrix Computations*, 3rd ed. Baltimore, MD, USA: The Johns Hopkins Univ. Press, 1996.

[41] A. Aho and J. Ullman, *Foundations of Computer Science*. New York, NY, USA: Computer Science Press, Inc., 1992.

[42] R. Jain, D.-M. Chiu, and W. R. Hawe, *A Quantitative Measure of Fairness and Discrimination for Resource Allocation in Shared Computer System*, vol. 38, Hudson, MA, USA: Eastern Research Laboratory, Digital Equipment Corporation Hudson, 1984.

[43] M. Grant. (2016). *CVX Forum: How to Express This Objective Function in CVX*. [Online]. Available: http://ask.cvxr.com/t/how-to-express-this-objective-function-in-cvx/637

IRFAN AHMED (M'10–SM'16) received the B.E. degree in electrical engineering and the M.S. degree in computer engineering from the University of Engineering and Technology, Taxila, Pakistan, in 1999 and 2003, respectively, and the Ph.D. degree in telecommunication engineering from the Beijing University of Posts and Telecommunications, Beijing, China, in 2008.

He was a Post-Doctoral Fellow with Qatar University from 2010 to 2011, where he was involved in two research projects, wireless mesh networks with Purdue University, USA, and radio resource allocation for LTE with Qtel. He was also involved in National ICT Pakistan funded research project Design and Development of MIMO and Cooperative MIMO Test-Bed with Iqra University, Islamabad, Pakistan, from 2008 to 2010. He is currently an Associate Professor with Taif University, KSA. He has authored over 25 international publications. His research interests include wireless LAN medium access control protocol design and analysis, cooperative communications, MIMO communications, performance analysis of wireless channels, energy constrained wireless networks, cognitive radio networks, and radio resource allocation.

Dr. Ahmed served as the Session Chair of the IEEE Wireless Communications, Networking and Mobile Computing conference held in Shanghai, China, in 2007, and the IEEE ICC 2016. He is an active Reviewer of the IEEE, Springer, and Elsevier journals, and conferences. He is an Associate Editor of the IEEE Access journal.

HEDI KHAMMARI received the B.Eng. and M.Eng. degrees in electrical engineering with automatic control specialization, and the Ph.D. degree in electrical engineering from the Tunis University, Tunis, in 1988, 1990, and 1999, respectively. He is currently an Associate Professor with the Department of Computer Engineering, College of Computers and Information Technology, Taif University, Saudi Arabia.

ADNAN SHAHID (M'15) received the B.Eng. and M.Eng. degrees in computer engineering with communication specialization from the University of Engineering and Technology, Taxila, Pakistan, in 2006 and 2010, respectively, and the Ph.D. degree in information and communication engineering from Sejong University, South Korea, in 2015. From 2007 to 2012, he was a Lecturer in electrical engineering with the Department of National University of Computer and Emerging Sciences, Pakistan. From 2012 to 2015, he was a Ph.D. Research Assistant with Sejong University. In 2015, he was a Post-Doctoral Researcher with Yonsei University, South Korea. From 2015 to 2016, he was with the Department of Computer Engineering, Taif University, Saudi Arabia. He is currently a Post-Doctoral Researcher with iMinds/IBCN, Department of Information Technology, University of Ghent, Belgium. He is coordinating and actively involved in the research activities of the research project eWINE funded by the European Commission under the Horizon2020 Program. He actively involved in various research activities. He was a recipient of the prestigious BK 21 plus Postdoc Program at Yonsei University. He is serving as an Associate Editor of the IEEE Access Journal.

His research interests include the next generation wireless communication and networks with prime focus on resource management, interference management, cross-layer optimization, self-organizing networks, small cell networks, device to device communications, machine to machine communications, and 5G wireless communications.